



Supplement of

Submicron aerosol source apportionment of wintertime pollution in Paris, France by Double Positive Matrix Factorization (PMF²) using Aerosol Chemical Speciation Monitor (ACSM) and multi-wavelength Aethalometer

J.-E. Petit et al.

Correspondence to: J.-E. Petit (jean-eudes.petit-etudiant@ineris.fr)

Supplementary Materials

Submicron aerosol source apportionment of wintertime pollution in Paris, France by Double Positive Matrix Factorization (PMF2) by using Aerosol Chemical Speciation Monitor (ACSM) and multi-wavelength Aethalometer

J.-E. Petit^{1, 2}, O. Favez¹, J. Sciare², F. Canonaco³, P. Croteau⁴, G. Močnik⁵, J. Jayne⁴, D. Worsnop⁴, E. Leoz-Garziandia¹

[1]{Institut National de l'Environnement Industriel et des RISques, INERIS, Parc Technologique ALATA BP2, 60550 Verneuil-en-Halatte, France}

[2]{ Laboratoire des Sciences du Climat et de l'Environnement, LSCE, UMR8212, CNRS-CEA-UVSQ, 91191 Gif-sur-Yvette}

[3]{Laboratory of Atmospheric Chemistry, Paul Scherrer Institute, 5232 PSIVilligen, Switzerland}

[4]{Aerodyne Research, Inc. 45 Manning Road Billerica, MA, USA}

[5]{Aerosol d.o.o., Kamniška 41, SI-1000 Ljubljana, Slovenia}

Correspondence to: J.-E. Petit (jean-eudes.petit-etudiant@ineris.fr)

Appendix A. Aethalometer model

Introduced by Sandradewi et al. (2008), the deconvolution of Black Carbon concentrations into its two main constituents (wood burning and fossil fuel) is based on i) the fact that black carbon is emitted only from the two aforementioned combustion sources; and ii) enhanced absorption of wood combustion in ultraviolet wavelengths due to emission of Polycyclic Aromatic Hydrocarbons (PAH) and humic-like substances (HULIS). Multi-wavelengths Aethalometer measurements highlight of the absorption spectral dependence and thus allow for such a deconvolution.

Absorption coefficients can be related to wavelengths and absorption coefficients of traffic and wood burning conditions (eq. A.1, A.2, A.3, A.4).

$$\frac{b_{abs}(\lambda_{UV})_{wb}}{b_{abs}(\lambda_{IR})_{wb}} = \left(\frac{\lambda_{UV}}{\lambda_{IR}}\right)^{-\alpha_{wb}} \quad (\text{A.1.})$$

$$\frac{b_{abs}(\lambda_{UV})_{ff}}{b_{abs}(\lambda_{IR})_{ff}} = \left(\frac{\lambda_{UV}}{\lambda_{IR}}\right)^{-\alpha_{ff}} \quad (\text{A.2.})$$

$$b_{abs}(\lambda_{UV}) = b_{abs}(\lambda_{UV})_{wb} + b_{abs}(\lambda_{UV})_{ff} \quad (\text{A.3.})$$

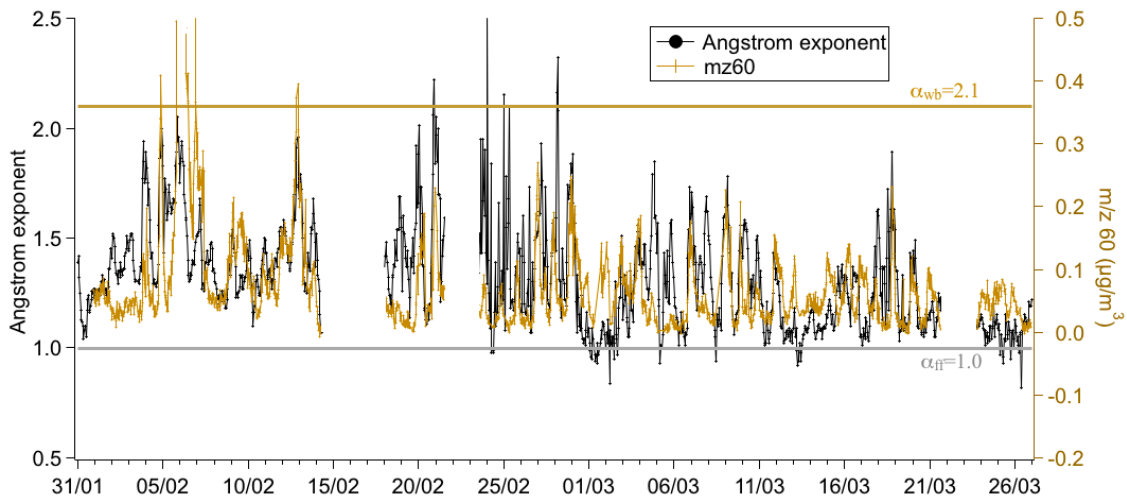
$$b_{abs}(\lambda_{IR}) = b_{abs}(\lambda_{IR})_{wb} + b_{abs}(\lambda_{IR})_{ff} \quad (A.4.)$$

2

3 In the case of this study, the 470 nm and the 950 nm channels were used in the calculation, as
 4 well as an absorption coefficient of 2.1 and 1.0 for pure wood burning and traffic,
 5 respectively. Fig. A.1. illustrates the choice α_{wb} . Besides a noticeable correlation between the
 6 Angstrom exponent and m/z 60 (tracer of levoglucosan), pure and local (i.e. fresh) wood
 7 burning condition is observed during the night of the 5th - 6th February (as described in the
 8 discussion paper), where the Angstrom exponent reaches 2.06.

9 Diurnal patterns of the two BC components correspond very well to the expected emission
 10 dynamics of the traffic and wood-burning source (Fig. A.2.). BC_{ff} presents a clear peak during
 11 the morning and a broaden peak during the evening; and BC_{wb} exhibits a peak during evening
 12 hours.

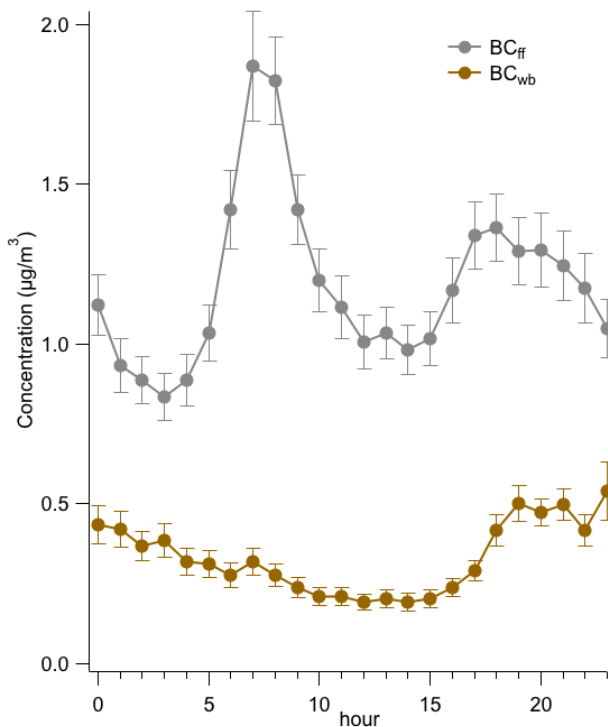
13



14

15 Figure A.1. Timeseries of the absorption Angstrom exponent and m/z 60 (referring to
 16 levoglucosan fragmentation) from the ACSM.

17



18

19 Figure A.2. Diurnal variations of BC_{wb} and BC_{ff}

1
2

1 **Appendix B. Choosing the appropriate number of factors**

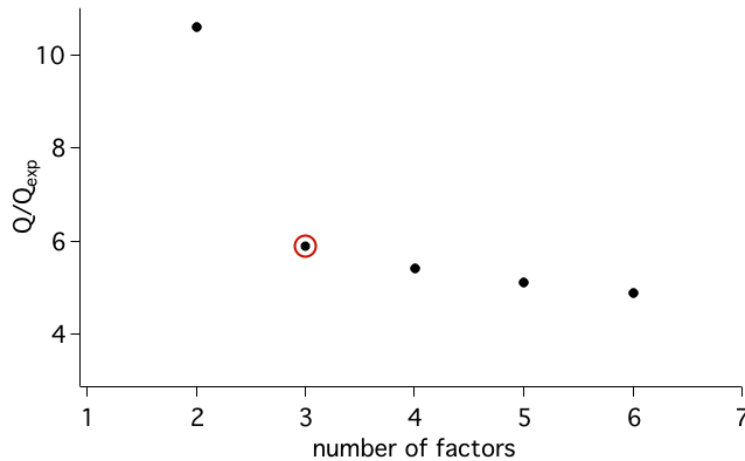
2 OA source apportionment

3

4 The appropriateness of OA source apportionment solutions was investigated by varying the
5 numbers of factors from 2 to 6. The most obvious change of Q/Q_{exp} slope occurs at 3 factors,
6 indicating that the 3-factor solution is appropriate (Fig. B.1).

7 The 4-factor solution presents two splitted BBOA factors, the sum of the two correlating very
8 well to BBOA of the 3-factor solution ($r^2=0.96$).

9

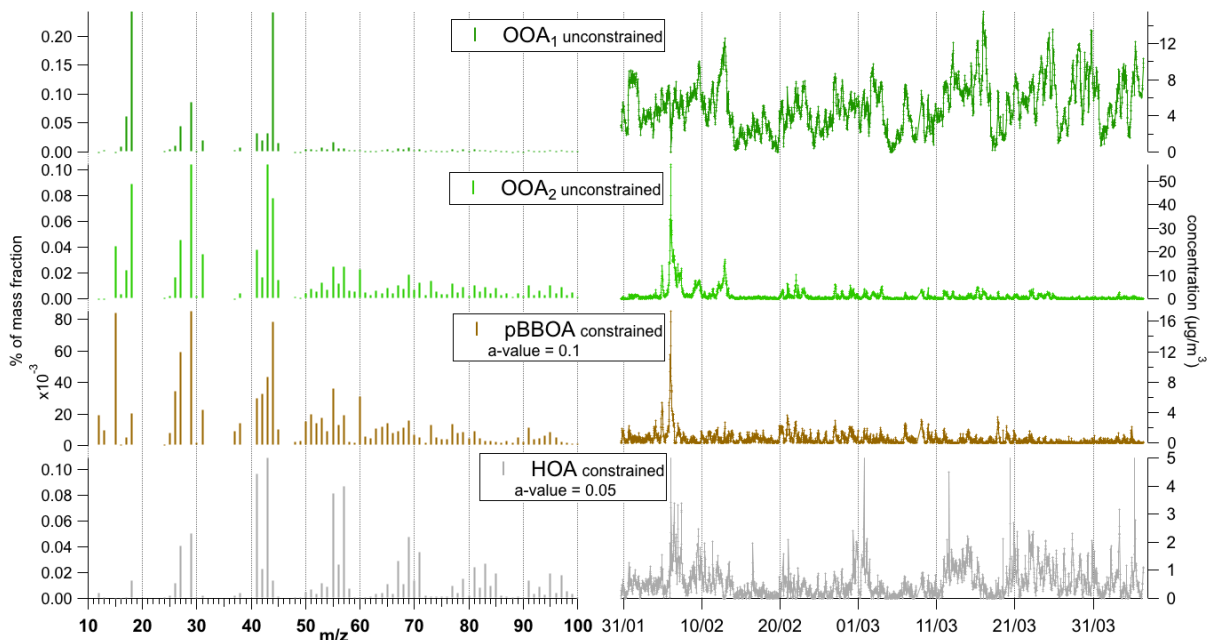


10

11

12 Figure B.1. Q/Q_{exp} variations over different number of factors

13



14

15 Figure B.2. Factor profiles and timeseries for the 4-factor solution

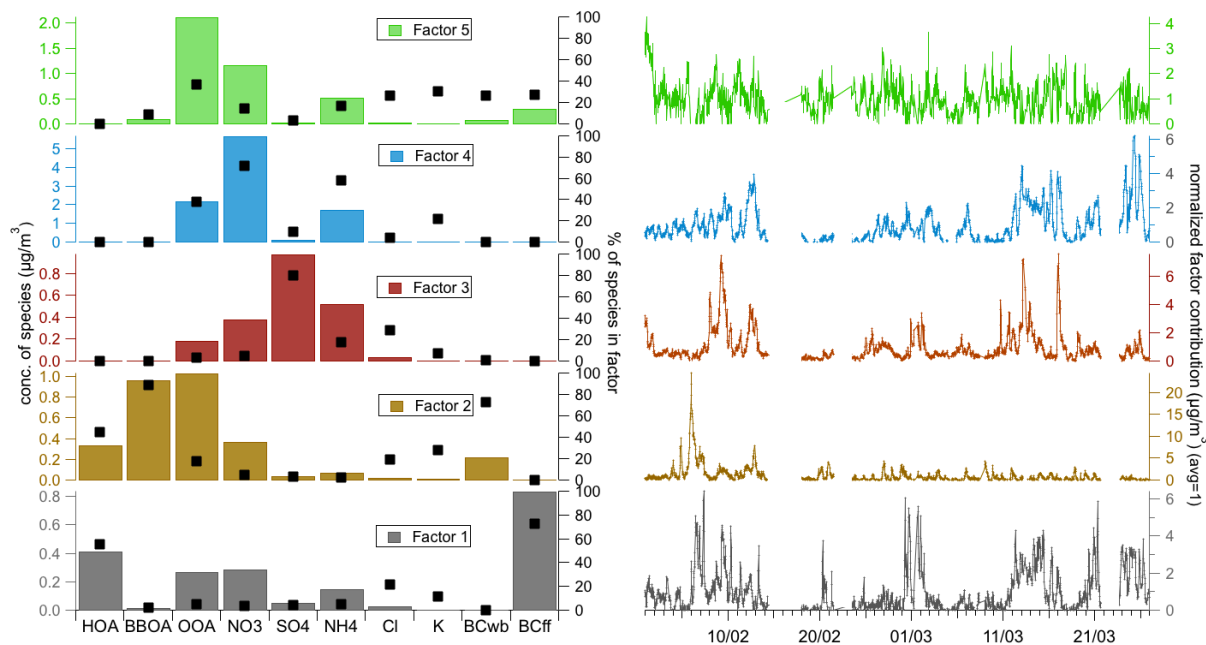
16

17 PM₁ source apportionment

18 Similarly, increasing the number of factors in the global PM₁ source apportionment leads to
19 noisy and unstable factors. The 5-factor solution presents two splitted semi-volatile secondary

1 aerosol factors, dominated by OOA and ammonium nitrate (Fig. B.3.). Moreover, bootstrap
 2 calculations (Table B.1.) highlight a lower stability of the fifth factor, making the 4-factor
 3 solution more appropriate.

4



5

6 Figure B.3. Factor profiles (left) and time-series (right) of the 5-factor solution

7 Table B.1. Bootstrap mapping of the 5-factor solution from the global PM₁ source
 8 apportionment analysis.

% of bootstrap mapping	Factor 1	Factor 2	Factor 3	Factor 4	Factor 5	Unmapped
Factor 1	100	0	0	0	0	0
Factor 2	0	100	0	0	0	0
Factor 3	0	0	100	0	0	0
Factor 4	0	0	0	100	0	0
Factor 5	2	15	0	0	77	6

9

10

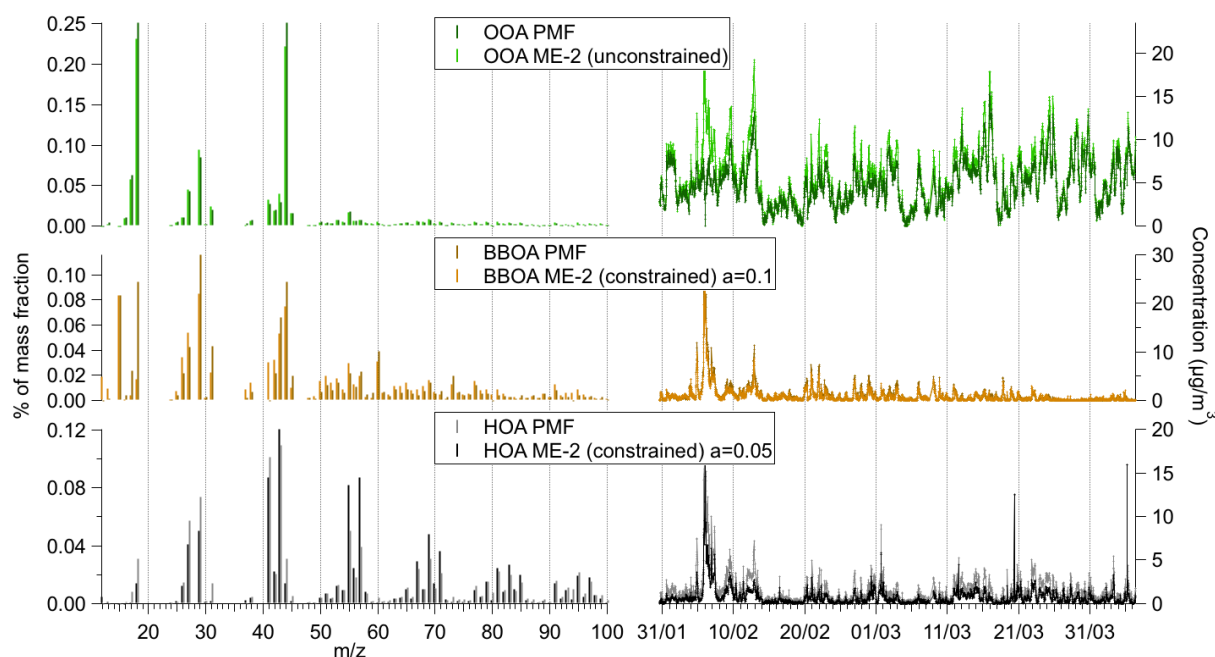
1 Appendix C. Comparison between unconstrained and constrained PMF analysis

2 An unconstrained PMF analysis was carried out prior to ME-2 constrained analysis. As
3 obtained further with constrained ME-2, this PMF analysis led to a 3-factor solution;
4 Comparisons between both output datasets are illustrated and summarized in Fig. C.1. and
5 Table C.1. Only slight differences are noticeable with time-series and profiles correlation
6 coefficient (r^2) being higher than 0.85 and 0.72 respectively. The lowest correlation is
7 observed for BBOA factor profile ($r^2=0.72$), but does surprisingly not have an influence on
8 factor timeserie ($r^2=0.98$). A same feature is observed for HOA outputs (correlation
9 coefficient of 0.83 and 0.95 for factor profile and timeserie respectively). This can be
10 explained by the proximity of BBOA and HOA profiles (at least for some of the major m/z)
11 but clearly distinct diurnal patterns (Lanz et al., 2007).

12 The OOA factor timeserie from the unconstrained analysis presents an unrealistic temporal
13 variation around February 6th, with a clear drop of modeled concentrations at the same time as
14 intense peaks of BBOA and HOA, suggesting that constrained runs were more appropriate.
15 An investigation of the influence of this episode is presented in Appendix F.

16 Although discrepancies in the variability of timeseries are low, changes in slopes (Table C.1.)
17 alter signal-to-noise ratios and could then influence the results of a subsequent PMF analysis.
18 The PMF² methodology was then applied using the OA factors from unconstrained analysis.

19



20

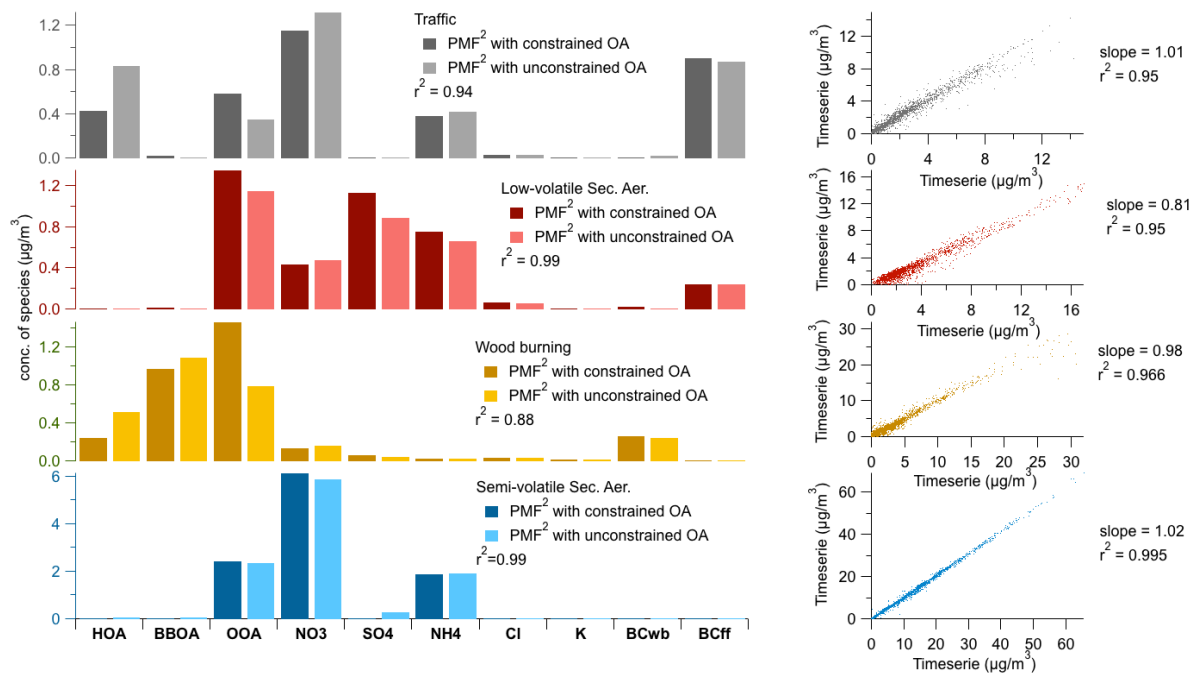
21 Figure C.1. Factor profiles (left) and timeseries (right) of unconstrained and constrained runs
22 during the 2012 late winter period in Paris.

23

1 Table C.1. Pearson correlations and slopes between constrained and unconstrained factor
 2 profiles and timeseries.

	HOA		BBOA		OOA	
	profile	timeserie	profile	timeserie	profile	timeserie
r^2	0.83	0.95	0.72	0.98	0.99	0.85
slope		0.81		1.26		1.61

3



4

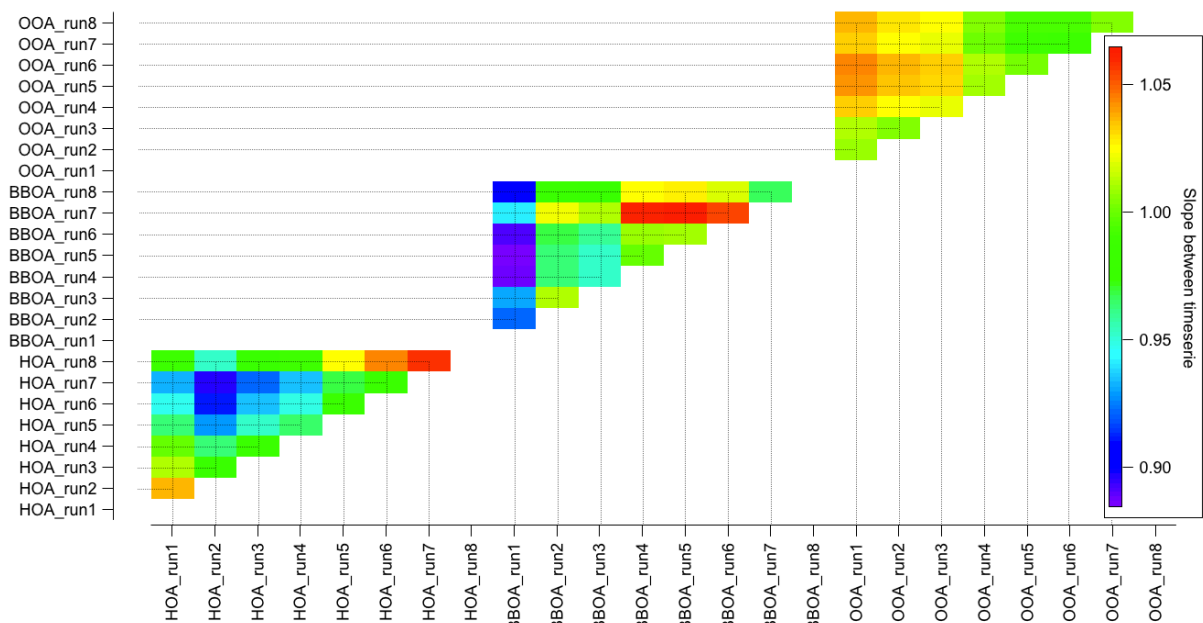
5 Figure C.2. Factors profiles (left) and timeseries scatter plot (right) of the PMF² analysis using
 6 OA factors from constrained and unconstrained PMF analysis

7

1 **Appendix D. Sensitivity tests on a-values chosen within OA source apportionment**

2 As performed in Lanz et al.(2008), and in order to investigate the role of a-values into the
3 ME2 analysis, several constrained PMF analysis were performed using different a-values for
4 BBOA and HOA reference profiles, from 0.05 to 0.80 (Table D.1.). Comparison of timeseries
5 is showed in Fig. D.1 and D.2. For BBOA profile, correlation coefficients are always higher
6 than 0.99, and slopes vary from ~0.90 to ~1.03, highlighting the poor influence of a-value
7 variations. Higher discrepancies are observed within the variation of a-values for the HOA
8 profile. However, Pearson coefficients remains satisfactory (higher than 0.98), and slopes
9 vary from ~0.70 to ~1.10, but interestingly stay in the range of 30% relative uncertainty input
10 for the global PM source apportionment analysis (Table 1 of the discussion paper).

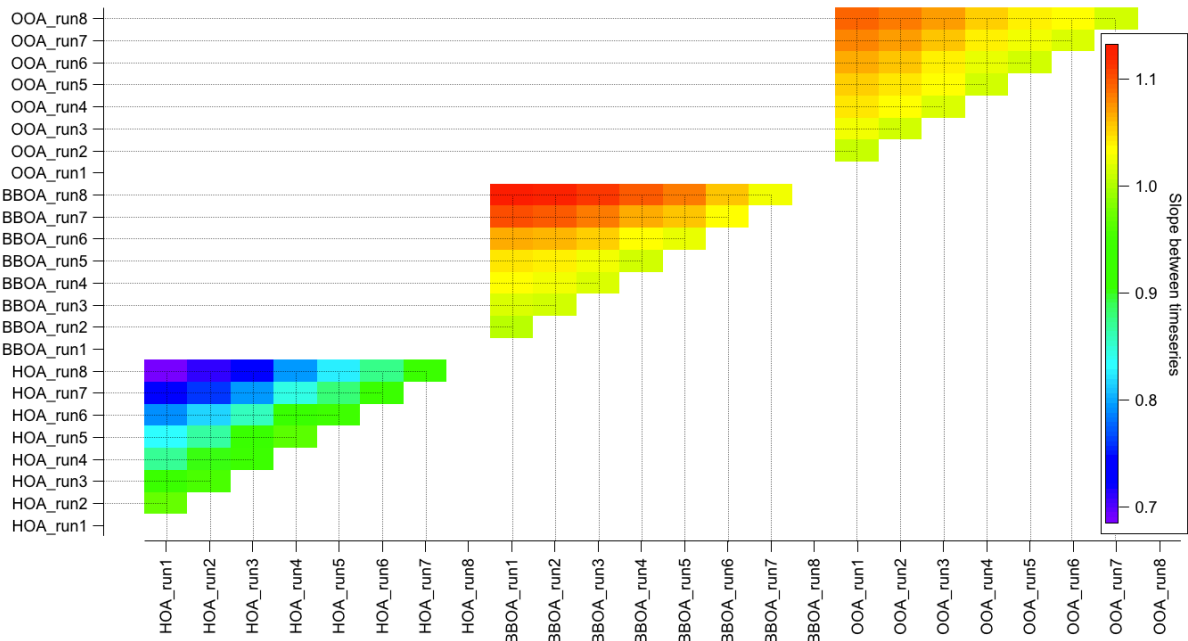
11



12

13 Figure D.1. Surface plot of slopes between timeseries using different a-values for BBOA
14 constrained profile. All Pearson coefficients were higher than 0.99.

15



1

2 Figure D.2. Surface plot of slopes between timeseries using different a-values for HOA
 3 constrained profile. All Pearson coefficients were higher than 0.98.

4

5 Table D.1. Parameters for a-value investigational runs

Run #	1	2	3	4	5	6	7	8
a-value BBOA	0.1	0.2	0.3	0.4	0.5	0.6	0.7	0.8
a-value HOA	0.05	0.1	0.2	0.3	0.4	0.5	0.6	0.7

6

7

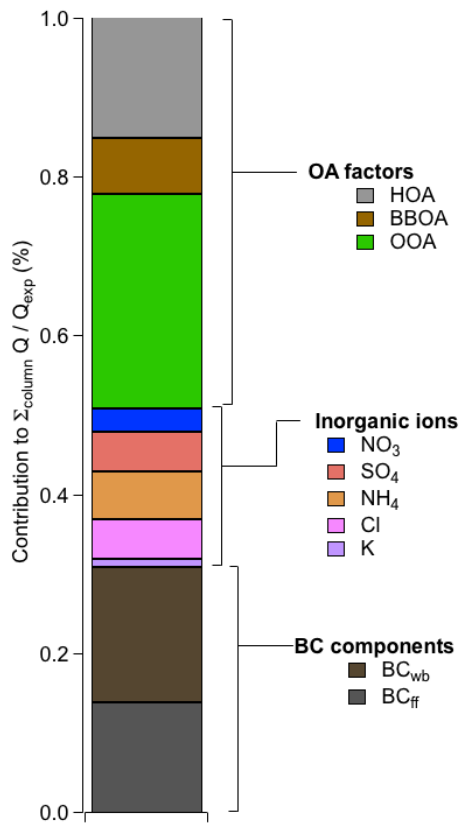
1 **Appendix E. Influence of the uncertainties used in the PM₁ source apportionment**

2 Defining uncertainties of variables is one of the most important key-point prior to a PMF
3 analysis. As OA factors present highest contribution to the Q/Q_{exp} ratio (49%) in the PM₁
4 source apportionment (Fig. E.1.), their impact on the quality of the factorization was
5 investigated by varying their relative uncertainty (in %) in the error matrix, calculated from
6 Polissar et al. (1998). Increasing the uncertainty of OA factors from 20% to 50% (Fig. E.2.)
7 does not have a significant impact on the variation of the Q for HOA, BBOA and NH₄; leads
8 to a fairly constant decrease of Q for SO₄ and the two BC components. And for OOA and
9 NO₃, a two-step decrease is observed with a change of slope between 30% and 40%, meaning
10 that this range of uncertainty leads to optimized fitting and minimized residuals, even though
11 their thorough determination is not possible yet for reasons explained in the discussion paper.

12 Results of the PM₁ source apportionment using $u_{\text{OA}}=30\%$ or 40% are very similar (Fig. E.3.)
13 with coefficients of correlation greater than 0.9 for profiles and timeseries. Slopes between
14 timeseries are very close to 1 except for the Traffic source where the $u_{\text{OA}}=40\%$ solution
15 presents an underestimation of 21%, mostly due to lower concentrations of ammonium nitrate
16 in the factor profile. It is however important to note that the $u_{\text{OA}}=30\%$ solution best fitted the
17 total mass (sum of each variables), with a slope of 1.004 (compared to 0.98 with $u_{\text{OA}}=40\%$).

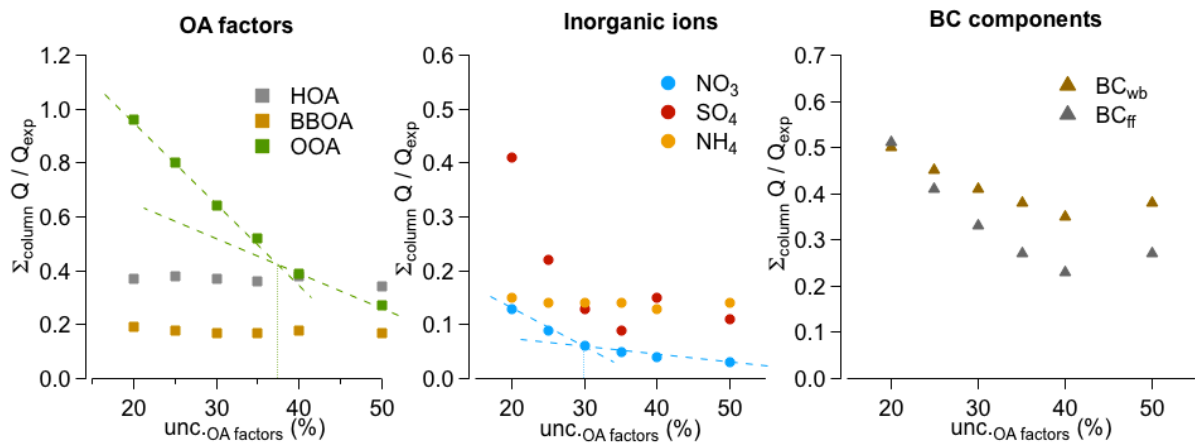
18 Similarly, changing the uncertainty of the two BC components from 40% to 20% does not
19 have a significant impact on factor profiles and timeseries (Table E.1.), as the latter as specific
20 tracers of two distinct sources.

21 Finally, increasing the uncertainty of the inorganic ions (NO₃⁻, SO₄²⁻, NH₄⁺ and Cl⁻) from
22 15% to 40% leads to unstable solutions, where bootstrap analysis is not satisfactory (Table
23 E.2.), and sulfate particularly badly modeled during pollution episodes.



1

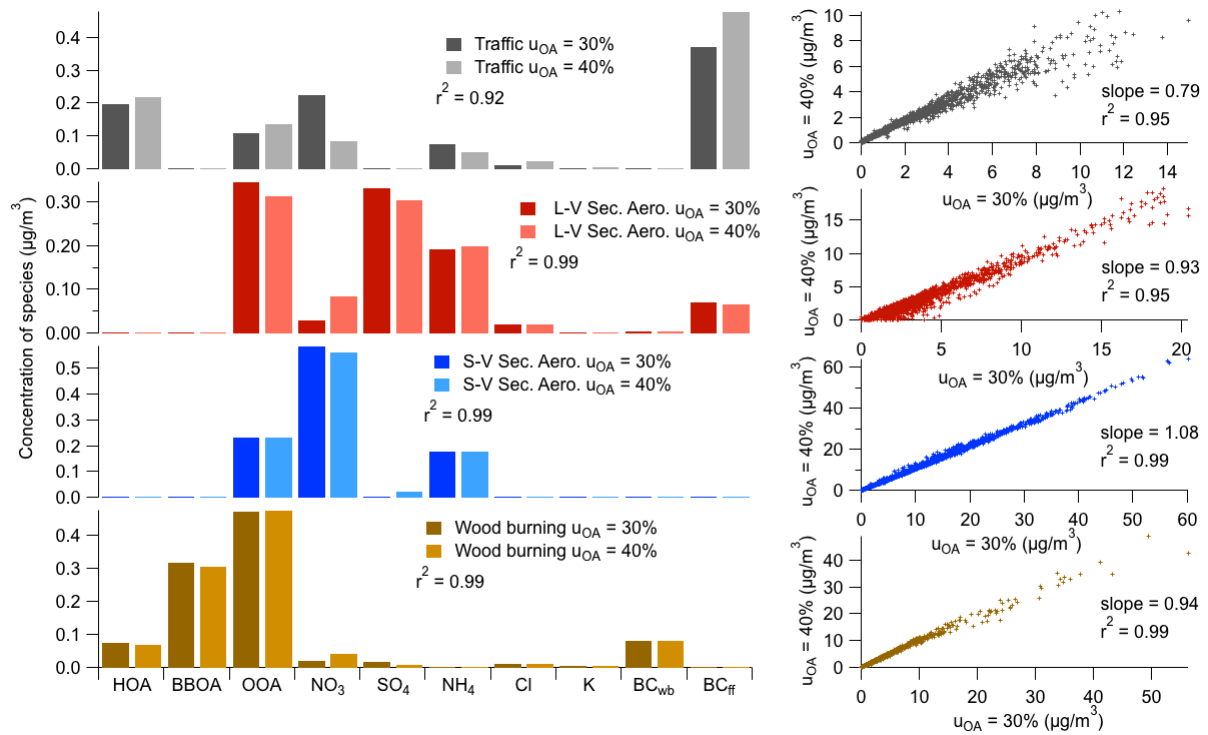
2 Figure E.1. Contribution to the total Q/Q_{exp} of each variable of the PM_{10} source apportionment



3

4 Figure E.2. Sum of the Q/Q_{exp} ratio for each variable with different uncertainties for OA
5 factors

6



1

2 Figure E.3. Comparison of factor profiles and timeseries from the PM₁ source apportionment
 3 using $u_{OA} = 30\%$ and 40%

4

5 Table E.1. Comparison (slopes and r^2) of factor profiles and timeseries when using an
 6 uncertainty for the BC components of 20% instead of 40%.

	Wood burning		Traffic		SV-Sec. Aer.		LV-Sec. Aer	
	slope	r^2	slope	r^2	slope	r^2	slope	r^2
timeseries	0.94	0.99	1.01	0.93	0.94	0.99	1.06	0.96
profiles		0.99		0.94		0.99		0.99

7

1 Table E.2. Bootstrap mapping of 4-factor solution using an uncertainty for the inorganic ions
 2 of 40% instead of 15%.

% of bootstrap mapping	Base LV-SA	Base Traffic	Base SV-SA	Base Wood Burning	Unmapped
Boot LV-SA	69	0	3	2	26
Boot Traffic	0	100	0	0	0
Boot SV-SA	0	0	98	0	2
Boot Wood Burning	0	0	0	100	0

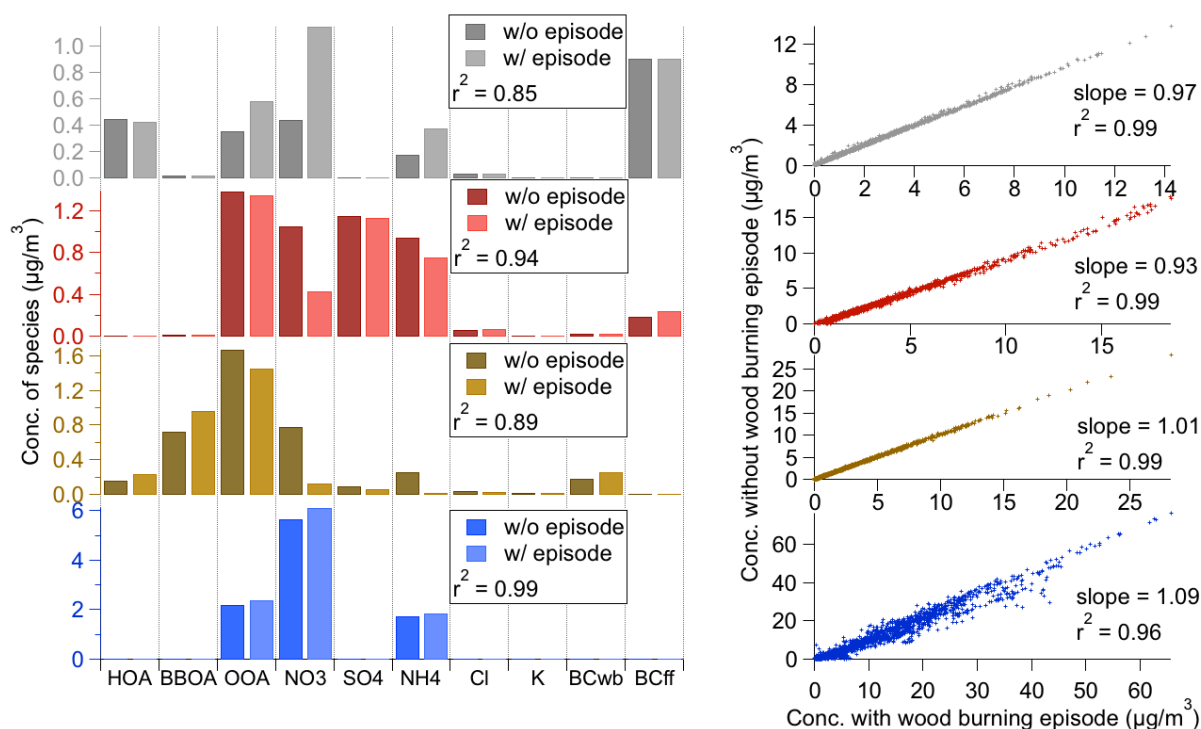
3

4

1 **Appendix F. Comparison between the double PMF analysis with and without the intense**
 2 **initial Wood Burning episode(February 6th).**

3 As suggested by Norris et al. (2008), intense, sharp and sporadic events (e.g. fireworks) are
 4 usually put aside from any PMF analysis because of the non-representativeness of the source
 5 over the whole database. In our case, on the 6th of February, an intense peak of organic
 6 concentration is observed and can be linked to wood burning emissions. The influence of this
 7 episode on results presented in the manuscript is investigated here by performing the same
 8 double PMF analysis excluding this peak. OA source apportionment and global PM₁ source
 9 apportionment were thus redone starting on February 7th. The comparison of profiles and
 10 timeseries is presented in Fig. F.1. Although some discrepancies are observed for factor
 11 profiles ($r^2 > 0.85$), especially with different nitrate proportions, factor timeseries are very
 12 consistent to each other ($r^2 > 0.96$) and present slopes close to 1. Therefore, the wood-burning
 13 episode observed on February 6th is assessed to have only little impact on final results.

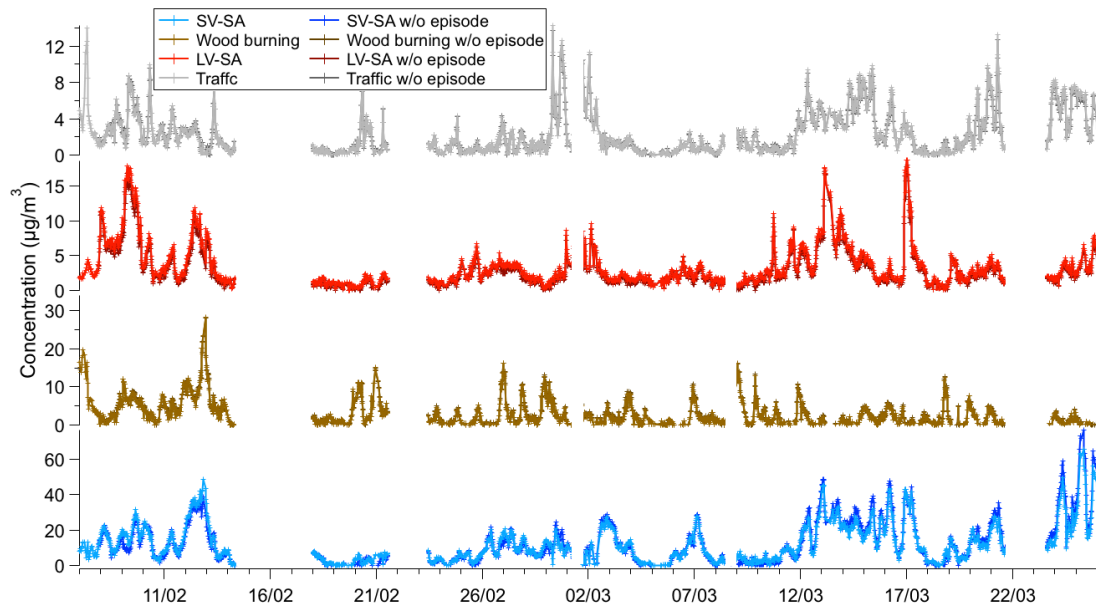
14



15

16 Figure E.1. Comparison of factor profiles and timeseries from the double PMF analysis when
 17 ex-/including the wood burning episode on February 6th.

18



1

2 Figure F.2. Timeseries from the double PMF analysis when ex-/including the wood burning
 3 episode on February 6th

4

1 **References**

- 2 Lanz, V. A., Alfarra, M. R., Baltensperger, U., Buchmann, B., Hueglin, C. and Prevot, A. S.
3 H.: Source apportionment of submicron organic aerosols at an urban site by factor analytical
4 modelling of aerosol mass spectra, , 7, 1503–1522, 2007.
- 5 Lanz, V. A., Alfarra, M. R., Baltensperger, U., Buchmann, B., Hueglin, C., Szidat, S., Wehrli,
6 M. N., Wacker, L., Weimer, S. and Caseiro, A.: Source attribution of submicron organic
7 aerosols during wintertime inversions by advanced factor analysis of aerosol mass spectra,
8 *Environ. Sci. Technol.*, 42(1), 214–220, 2008.
- 9 Norris, G. A., Vedantham, R., Wade, K., Brown, S., Prouty, J. and Foley, C.: EPA Positive
10 Matrix Factorization (PMF) 3.0: Fundamentals & User Guide, U.S. Environmental Protection
11 Agency. [online] Available from:
12 http://www.epa.gov/heads/documents/EPA_PMF_3.0_User_Guide.pdf (Accessed 20
13 February 2014), 2008.
- 14 Polissar, A. V., Hopke, P. K., Paatero, P., Malm, W. C. and Sisler, J. F.: Atmospheric aerosol
15 over Alaska: 2. Elemental composition and sources, *J. Geophys. Res. Atmospheres*,
16 103(D15), 19045–19057, doi:10.1029/98JD01212, 1998.
- 17 Sandradewi, J., Prévôt, A. S. H., Szidat, S., Perron, N., Alfarra, M. R., Lanz, V. A.,
18 Weingartner, E. and Baltensperger, U.: Using Aerosol Light Absorption Measurements for
19 the Quantitative Determination of Wood Burning and Traffic Emission Contributions to
20 Particulate Matter, *Environ. Sci. Technol.*, 42(9), 3316–3323, doi:10.1021/es702253m, 2008.

21